Environment and Ecology Research 11(2): 340-361, 2023
DOI: 10.13189/eer.2023.110209 http://www.hrpub.org

Removal of Lead Ions from Aqueous Media Using Rice Husk Modified with Manganese Oxide

Ta Thi Huong*, Tran Y Doan Trang

Haui Institute of Technology, Hanoi University of Industry, Vietnam

Received November 26, 2022; Revised March 8, 2023; Accepted April 7, 2023

Cite This Paper in the Following Citation Styles

(a): *[1] Ta Thi Huong, Tran Y Doan Trang , "Removal of Lead Ions from Aqueous Media Using Rice Husk Modified with Manganese Oxide," Environment and Ecology Research, Vol. 11, No. 2, pp. 340 - 361, 2023. DOI: 10.13189/eer.2023.110209.*

(b): *Ta Thi Huong, Tran Y Doan Trang (2023). Removal of Lead Ions from Aqueous Media Using Rice Husk Modified with Manganese Oxide. Environment and Ecology Research, 11(2), 340 - 361. DOI: 10.13189/eer.2023.110209.*

Copyright©2023 by authors, all rights reserved. Authors agree that this article remains permanently open access under the terms of the Creative Commons Attribution License 4.0 International License

Abstract The creation of effective adsorbents from agricultural waste to remove heavy metals such as toxic lead ions has been widely used. The goal of this research is to remove lead from water using rice husk-manganese oxide (RH-Mn). The raw rice husk was processed in three stages: (1) treatment with hydrochloric acid (HCl) 1M and sodium hydroxide (NaOH) 1M; (2) keep treating the material at the first stage in an ultrasonic water bath with a solution of 50 mL distilled water and 5 mL ethanol (90 ℃) plus 1,5g potassium permanganate ($KMnO_4$); (3) Continuously adding few drops of 10% hydro peroxide (H_2O_2) to the solution and stirring until the precipitation solid turns brown or black. The material was filtered and dried for 6 hours at 80^0C. Scanning electron microscopy (SEM), energy-dispersive X-ray spectroscopy (EDX), and X-ray diffraction (XRD) were used to determine MnO_2 and observe the differences between the raw rice husk and modified rice husk. Besides, batch adsorption tests were carried out to investigate the influence of time, pH, and adsorbent dose on the adsorption removal process. Particularly, several outstanding performances in the research are: (1) Based on the statistically experimental design and response surface method (RSM) were applied to improve the adsorption system; (2) Pseudo-second-order kinetics and Freundlich isotherm models were shown to be effective in explaining lead adsorption on RH-Mn; (3) The modified adsorbent took four hours to reach the adsorption equilibrium. Over 99% of lead ions were eliminated from water under ideal conditions if the pH of the water was 4, the initial concentration was 15 mg/L, the contact period was 3 hours, and the RH-Mn dose was 1.5 g/L. This research can aid in the development of novel bioengineered low-cost adsorbents.

Keywords Lead Ions, Rice Husk, Manganese Oxide, Adsorption, Response Surface Methodology

1. Introduction

Due to its exceptional qualities, including superior softness, ductility, insulation, and corrosion resistance, lead ion (Pb(II)) is widely utilized in various sectors, including paint, electrical equipment, welding, batteries, electrical insulating materials, vehicles, automobiles, fuel, cosmetics, ceramics, etc. [1, 2]. However, this metal is also widely recognized for being extremely poisonous, and both natural and human activities may cause it to enter the air, water, and soil directly or indirectly [3, 4]. As per human health effects, many Pb(II) exposure symptoms were widely recognized such as anemia, renal failure, cardiovascular damage, hematological, nervous system damage, and even death can result from lead poisoning [5-7]. Since, it is important to get rid of lead contamination, especially marine lead pollution. Current methods for removing Pb(II) include physical-chemical, chemical precipitation, coagulation and flocculation, ion exchange, reserve osmosis, electrochemical treatments, membrane filtration, evaporation, flotation, oxidation, and bio-sorption procedures [8–11]. However, most of these methods have some disadvantages in that they may be

inefficient, expensive, generate secondary pollution, or are ineffective at low metal concentration levels [12–14]. Therefore, there is a need to develop a cost-effective and economical method and simple to apply.

However, the majority of these techniques have certain drawbacks, including the possibility of inefficiency, high costs, the creation of secondary pollutants, or the inability to work at low metal concentration levels [12–14]. Consequently, a simple, inexpensive, and cost-effective solution must be created, which is known as the adsorption method [15]. Adsorbent materials are currently popular and are often made from leftover waste products from our own paddy field. One of the easily accessible waste items that are produced in large quantities after each harvest in many nations is rice husk. Numerous researchers have successfully changed rice husk and converted them into viable materials for heavy metal removal. Many heavy metal ions such as Zn^{2+} [16], Cd^{2+} [17], Hg^{2+}, Ni^{2+}; Cu^{2+} [19-20]. Whether in their nature or after modification in water, they were effectively eliminated using modified rice husk and other adsorbents [15, 16].

Rice husk is frequently converted into activated carbon or subjected to various acid treatments in order to make adsorbents [18]. Few studies, nevertheless, have coupled the substance with metal oxides including iron, aluminum, and manganese oxide for the adsorption of heavy metals from drinking water and wastewater. Due to their relatively high surface area, microstructure, and possession of OH-functional groups capable of interacting with metals, many studies often consider the most critical detergents of heavy metals in aqueous or wastewater [21]. However, the majority of these metal oxides can only be produced as hydroxides or gels that are suspended in water or as fine powders. Solid/liquid separation is challenging in these circumstances. Besides, vertical metal oxides are not suitable as filtration media because of their hydraulic conductivity [22]. Hence, coating manganese oxide on filter media can solve the problem. Some research has shown that coating manganese oxides synthesized by $KMnO_4$ and C_2H_5OH on agricultural wastes or other materials such as chitosan can remove heavy metals [23, 24]. Furthermore, rice husk was modified by sodium hydroxide can increase adsorption capacity [25]; normally, this material usually pre-treaties with acid and base to remove impurities and then makes it as carbonized rice husk; calcined rice husk; activated carbon from rice husk or silica gel [25, 26], etc. However, using rice husk modified with manganese oxide to remove Pb(II) from water has not been studied yet.

In addition, it has become increasingly common to use statistical and mathematical approaches to determine the impact. From that discovering the experimental optimization, and lowering the number of experiments. It is called Response Surface Methodology (RSM) and is applied in a variety of industries. Optimization studies have been often used in many studies such as sandalwood oil [27], activated carbon [28], and nano-scale materials for dye removal [29]. The application response surface methodology on Pb(II) removal was investigated with aspergillus niger [30], another material by novel superparamagnetic nanocomposite to remove Pb(II) [31], effective removal Cr(VI) using fungal biomass [28], acid dye adsorption onto activated carbon prepared from wild date stones [32]. The goal of this work was to develop a novel, reasonably priced adsorbent to remove Pb(II) from water. In addition, XRD, SEM, and EDX analyses were used to investigate the characterizations of untreated and novel adsorbents. In batch systems, researchers have also looked at how pH, contact duration, and dose concentration affect adsorption capacity. To maximize the Pb(II) removal effectiveness from water, the response surface approach was applied.

For the author's study, we created a new type of adsorbent by modifying rice husk with synthesized MnO_2, in which rice husk is as a carrier to remove lead ions in water. In particular, our study considered the complete removal of lead ions with a low concentration was about 20 mg/L. This is the main goal that we achieve after conducting the experiment. Besides, the study combined with the RSM method to propose the input factors to completely remove 15 mg/L of lead ions under the research conditions. This is a new point that most previous studies have focused on creating materials to remove large amounts of heavy metal ions in water. However, we used to that when the concentration of heavy metal ions in water is lower, the ability to completely remove it is more difficult than the concentration of large ions. Because of the low concentration of heavy metal ions, their distribution density in water is low, making it difficult to contact the adsorbent. Therefore, our research both aims to completely remove lead ions in water and study the optimal conditions.

2. Methodology

2.1. Metal Solution

Analytical grade materials were utilized for all the chemicals and reagents in the experiments and analysis. In order to avoid precipitation, a few drops of concentrated nitric acid (HNO_3) were added to the lead (II) nitrate [$Pb(NO_3)_2$] powder (from VMCGROUP, Vietnam) and distilled water mixture to create a Pb(II) stock solution (1000 mgL^{-1}). The initial pH of the working solution was adjusted by adding HNO_3 (0.1M) and NaOH (0.1M) solution. Chemicals were prepared for synthesizing manganese oxide to modify rice husk and to do the experiments: Hydrochloric acid 35% manufactured by Thermo Fisher Scientific India Pvt.Ltd; nitric acid 68% produced by Jisico-Korea; sodium hydroxide 99% provided by Tien Phat chemical company, Vietnam; kali permanganate 99% provided by Vietchem company, Vietnam; ethanol 96% made by Viet My Chemical factory-Vietnam, and hydrogen peroxide 30% from

Vietchem company, all solutions were prepared using distilled water.

2.2. Optimization Method

For monitoring the impact of functional variables, conventional techniques use one variable at a time. Although other parameters are preserved at their current levels, the studied parameter is modified in this optimization technique [15]. This method requires a lot of time-consuming and expensive tests, and it is unable to examine interacting effects between the variables [27-30]. The best mix of variables and their interactions have been found to be best identified by utilizing multivariate statistical approaches rather than the one variety method [26]. A group of mathematical and statistical methods known as the response surface methodology (RSM) are effective for examining the influence of several independent factors on the response [31, 32]. RSM is useful for both the design and optimization of processes as well as for enhancing already existing designs. This methodology, which derives from experimental methods and incorporates interactive effects among the variables, is more useful than the ways previously discussed since it shows the total impacts of the factors on the process. RSM was applied to optimize Pb(II) removal by Aspergillus niger. The results revealed that 96.21% Pb(II) elimination under the pH solution was 4.27; Pb(II) initial concentration was 30mg/L; niger dose was 2.17 g/L [30]. Response surface approach was used to optimize the manufacturing parameters for activated carbons from Tamarind wood by zinc chloride. The ideal activated carbon was reached by utilizing a 439℃ activation temperature, a 40-minute activation duration, and a 296% moisture content, yielding 45.26% carbon and 291.73 mg/g malachite green oxalate intake. The effect of reaction temperature on the yield of activated was also detected [33]. Furthermore, For the purpose of efficiently removing Cr (VI) using fungi-derived biomass, isotherm modeling, kinetic research, and experimental optimization techniques employing response surface methodology [34]. Overall, RMS method has been widely employed in many fields. Since in the present research authors utilized a powerful method to determine the ideal condition in Pb(II) removal by modified rice husk.

2.3. Preparation of Rice Husk Modified Manganese Oxide (RH-Mn)

Stage 1: Pre-treated raw rice husk:

Firstly, the rice husk was sieved to get an approximated size of 450 μm and then treat with HCl (1M) under the temperature was 70^0C for 24 hours to remove impurities and open the shield of the rice husk. Because these factors could affect the adsorption results. Secondly, the modified rice husk in the first stage was washed with distilled water carefully to remove acid and kept soaking with NaOH 0.1M for 1 hour. It was kept washed with distilled water until the pH reached neutral. Thirdly, the treated rice husk in the second step was dried at 80℃ overnight.

Stage 2: Prepared for the solution to synthesize MnO_2 and modified treated rice husk with the solution:

The treated rice husk (2 grams) in the first stage was added to the solution that contained 50 mL of distilled water with 50 mL of ethanol (90%) in a beaker (Solution 1). Next, added $KMnO_4$ (1.5 gram) to solution 1 and kept stirring the new solution (Solution 2) under laboratory conditions. Solution 2 was put into an ultrasonic water bath and left for 1 hour at room temperature. Then, H_2O_2 (10%) was slowly dropped into solution 2 until the solution turned brown or black precipitation solid [1], [2]. Finally, the last solution was filtered under the vacuum filtration machine. Besides, we separated the solution and the solid. The solid was dried at the temperature was 80℃ for 6 hours (Figure 1 in the supplementary materials).

2.4. Characteristics of Rice Husk Modified Manganese Oxide (RH-Mn)

The crystallographic structure, chemical composition, and physical properties of the adsorbents before and after modification were obtained and checked by using X-Ray diffraction (XRD) Ultima IV from Rigaku, USA. To examine the surface of the adsorbent and its elemental composition on it the Field Emission Scanning Electron Microscope (FE-SEM) JSM-6500 was used from JEOL Japan. It is mainly carried out in a high vacuum as gas particles are likely to impact the electron beam and the generated backscattered as well as secondary electrons, which are needed for imaging. Energy Dispersive X-ray spectroscopy (EDS) was used. EDS is known as an analytical method used to describe the chemical composition or elemental composition of a sample. It is built around the relationship between the X-ray excitation source and the sample. Its properties are largely due to the basic premise that each element has a unique atomic structure.

2.5. Adsorption Experiments

The observed concentration of lead ions was diluted from the stock solution (1000 mgL^{-1}) with distilled water, and the pH value was combined with a particular amount of RH-Mn before stirring at 120 rpm. The centrifuge was used to extract the suspension after equilibrium was attained.

The residual concentration was analyzed by AAS machine - Thermo Fisher Scientific iCE 3300 Atomic Absorption Spectrometers (AAS). Each sample was duplicated for each sample. The amount of metal ion adsorbed was calculated as Eq. (1) [3]:

$$\% \text{ Adsorption} = \frac{C_0 - C_e}{C_0} \times 100 \quad (1)$$

Where, C_0 and C_e are the initial and equilibrium

concentrations of the adsorbent, respectively.

The amount of metal ion (q_t at time t) adsorbed per unit mass of the adsorbent (M) is evaluated by using the following Eq. (2) [4]:

$$q_t = \frac{C_0 - C_t}{M} \times V \quad (2)$$

In which, C_t: lead ion concentration (mgL^{-1}) at time t min, V: The volume of initial metal ion in liter, M: the mass of adsorbent in gram.

Similarly, the adsorption capacity (q_e) was determined by using the mass balance Eq. (3):

$$q_e = \frac{C_0 - C_e}{M} \times V \quad (3)$$

Where q_e (mg/g) is the number of metal ions adsorbed onto the material at the equilibrium.

2.5.1. Isotherm and Kinetic Studies

Langmuir isotherm model, which is assumed that the adsorption takes place on monomolecular layer on the surface, its linearized form Eq. (4) is presented the plot between C_e and C_e/q_e [5], [6]:

$$\frac{C_e}{q_e} = \frac{1}{q_{max}}\frac{1}{K_L} + \frac{1}{q_{max}}C_e \quad (4)$$

Where q_{max}: the adsorption capacity (mg/g), K_L: the Langmuir constant (L/mg)

Freundlich isotherm model: representing an empirical model, the assumption that adsorption is independent of surface coverage on the homogenous surface [3], [6].

$$\log q_e = \log K_f + \frac{1}{n}\log C_e \quad (5)$$

Where K_f: Adsorption capacity, n: adsorption intensity

Dubinin-Radushkevich isotherm (D-R isotherm): It is an empirical adsorption model commonly used to distinguish physical and chemical adsorption by the average free energy value [7], [8]. Its linearized form is displayed in Eq. (6) below.

$$Lnq_e = Lnq_s - (K_{ad}\varepsilon^2) \quad (6)$$

Where q_e: Amount of adsorbate in the adsorbent at equilibrium time, q_s: The theoretical isotherm saturation capacity (mg/g), K_{ad}: Dubinin-Radushkevich isotherm constant (mol^2/kJ^2), ε^2: Dubinin-Radushkevich isotherm constant.

Temkin isotherm model: It is reasonable for multilayer adsorption with heterogeneous adsorbents. The thermal adsorption of the surface of the molecules decreases linearly instead of logarithms with coverage. It can be expressed by the plot between q_e and LnC_e (Eq. (7)) [3], [9].

$$q_e = \frac{RT}{b_t} LnK_t + \frac{RT}{b_t} LnC_e \quad (7)$$

Where K_t (L/mg) is the Temkin isotherm constant, b_t (J/mol) is a constant, which is relevant to the heat of sorption, and R (8.314 J/mol/K) is the gas constant.

Pseudo-first-order: Its equation is usually used in the form below Eq. (8) [10], [11]:

$$Log(q_e - q_t) = Logq_e - \frac{K_1 t}{2.303} \quad (8)$$

Where K_1: Rate constant, q_t and q_e: the amounts of adsorbed at time t and equilibrium (mg/g), respectively.

Pseudo-second order: it is a quadratic kinematic model. The rate of biological uptake is controlled by chemical uptake and rate with the second power of the active part of the active site. It is expressed by Eq. (9) [12], [13].

$$\frac{t}{q_t} = \frac{t}{K_2 q_e^2} + \frac{t}{q_e} \quad (9)$$

Where, K_2: rate constant for the Pseudo-second model (g/mg.h), q_t and q_e: the amounts of adsorbed at time t and equilibrium (mg/g), respectively.

3. Results and Discussion

3.1. XRD Result

Figure 1 shows the X-ray diffraction of RH-Mn. Some obvious vertices (211); (301) and (521) can be observed. They are also well consistent with MnO_2 [14], [15]. While other peaks represent MnO_2 which inadequately appears. The peaks are less high and sharpen the XRD sample, it indicates that MnO_2 crystals are formed short-range and poorly crystalline [16]. Also, it is not possible to observe the peaks of other phases or impurities, which indicates that the high impurity MnO_2 can be obtained by the above method. Furthermore, the formation of MnO_2 is uniformly formatted on rice husk.

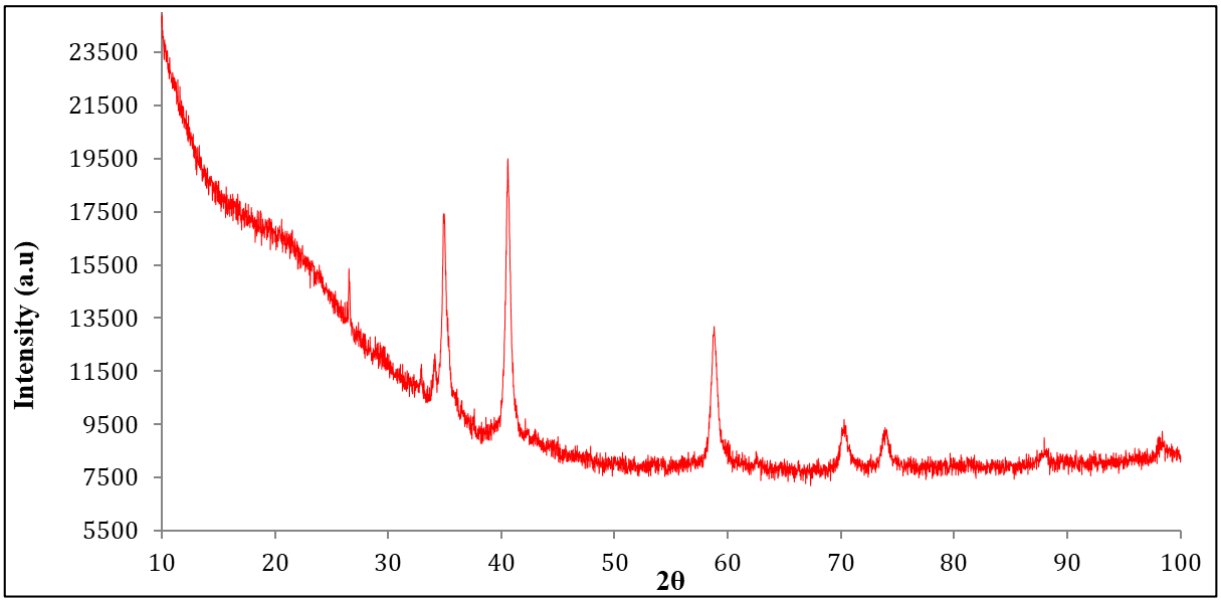

Note: 2θ is the angle of detector position from the incident X-Ray beam.

Figure 1. XRD of modified rice husk with manganese oxide (RH-Mn).

3.2. SEM/EDX Analysis

SEM is well-known as a technique for examining the material surface structure and morphological traits. Figure 2 depicts SEM pictures of pre-treated rice husk, acid-treated rice husk, and the synthesis of synthetic manganese oxide on rice husk. It was a thorough examination of how the surface altered at each level of treatment. Figure 2a shows a raw rice husk with a smooth surface and little cone designs that are naturally placed in sequential sequence. Without treatment, the surface of raw rice husk has uniform round-shaped hills and mimics the structure of a corncob. It does not promote adsorption. The shield underwent hydrochloric acid treatment, as shown in Figure 2b, and this resulted in the material's original surface being shattered. The surface of the hydrochloric acid-treated material becomes rougher; yet, the structure of the surface materials is uneven. On the material's surface, tiny holes may be seen, but the material's structure is still essentially intact. The shape of the manganese oxide layers that developed after being synthesized using tiny MnO_2 particle structures is shown in Figure 2c. As a result, the structure of the RH-Mn material becomes more porous, resulting in a considerable increase in the material's surface area. This is what has led to RH-Mn increased adsorption capability. MnO_2 nanostructure may be seen in the particle size, which is around 100 nm in diameter.

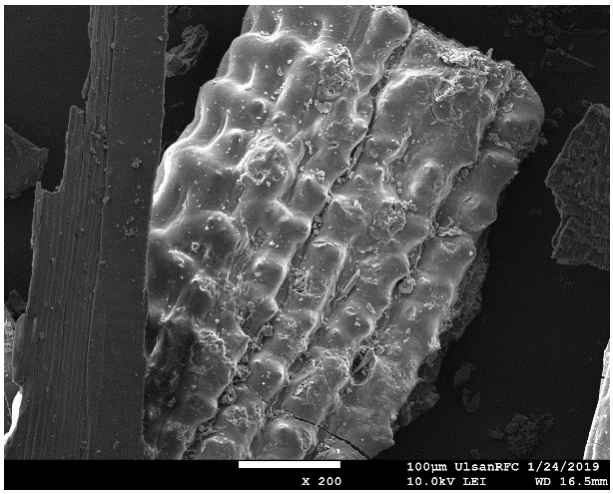

(a)

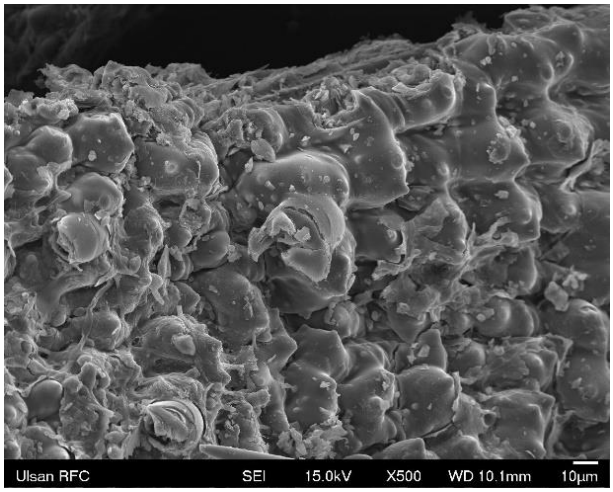

(b)

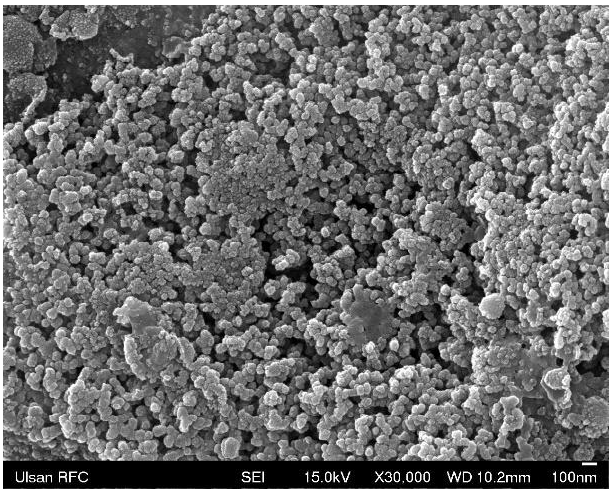

(c)

Figure 2. **(a)** SEM of raw rice husk; **(b)** rice husk treated by HCl; **(c)** synthesized manganese oxide coated rice husk (RH-Mn).

In a similar manner, Figure 3 depicts the 3D surface structures of RH-Mn and raw rice husk. The average surface elevation of the raw rice husk, which was rather homogeneous and measured at 159.4 on the color scale, showed that the milling operation had not significantly harmed the origin adsorbent on the shield (Figure 3a). The drastically altered surface caused by the synthetic RH-Mn process, however, may be well supported by Figure 3b. It is clear that the RH-Mn surface is characterized by many pointed columns of varying heights. They form multiple large, deep surface holes after swarming tightly together. It is a great indication for anticipating expected adsorption removal effectiveness. Additionally, the adsorption will benefit greatly and favorably from the presence of micro- and mesopores with rough surfaces.

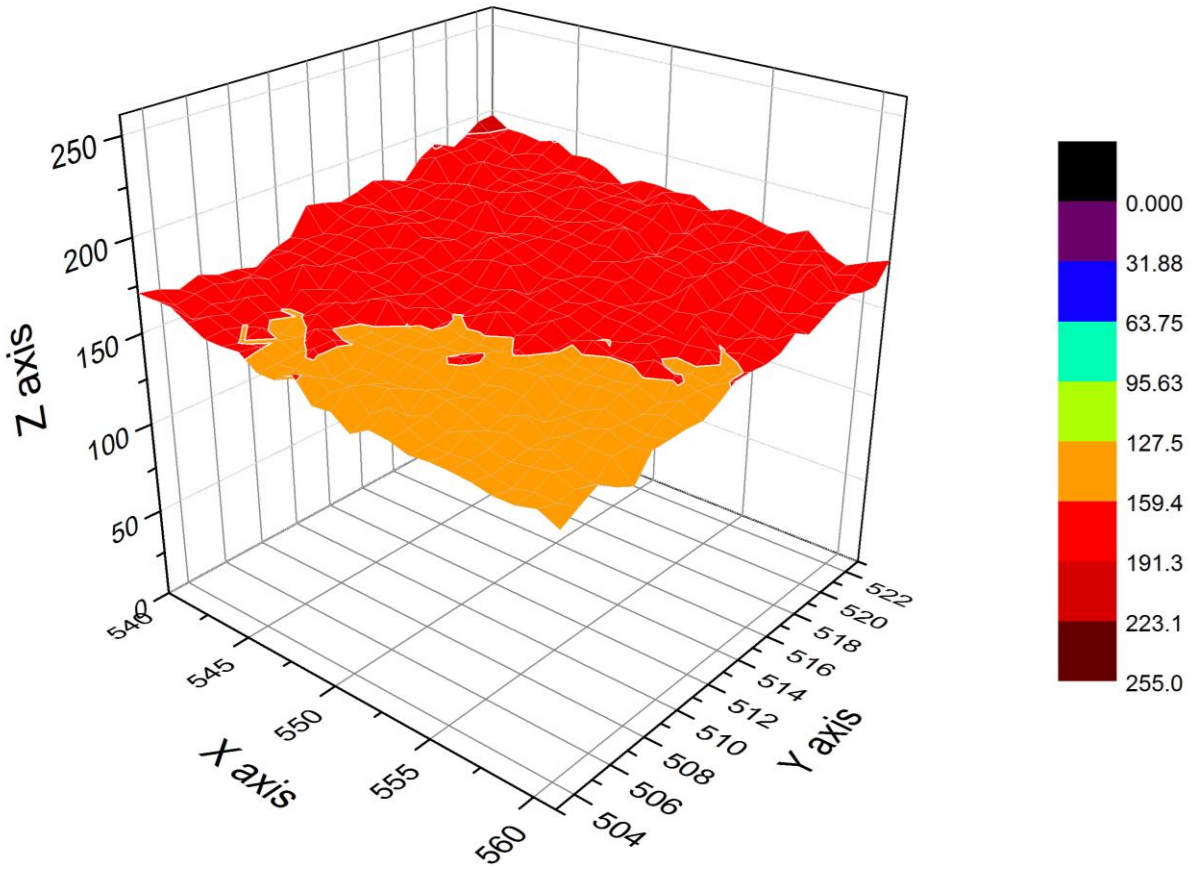

(a)

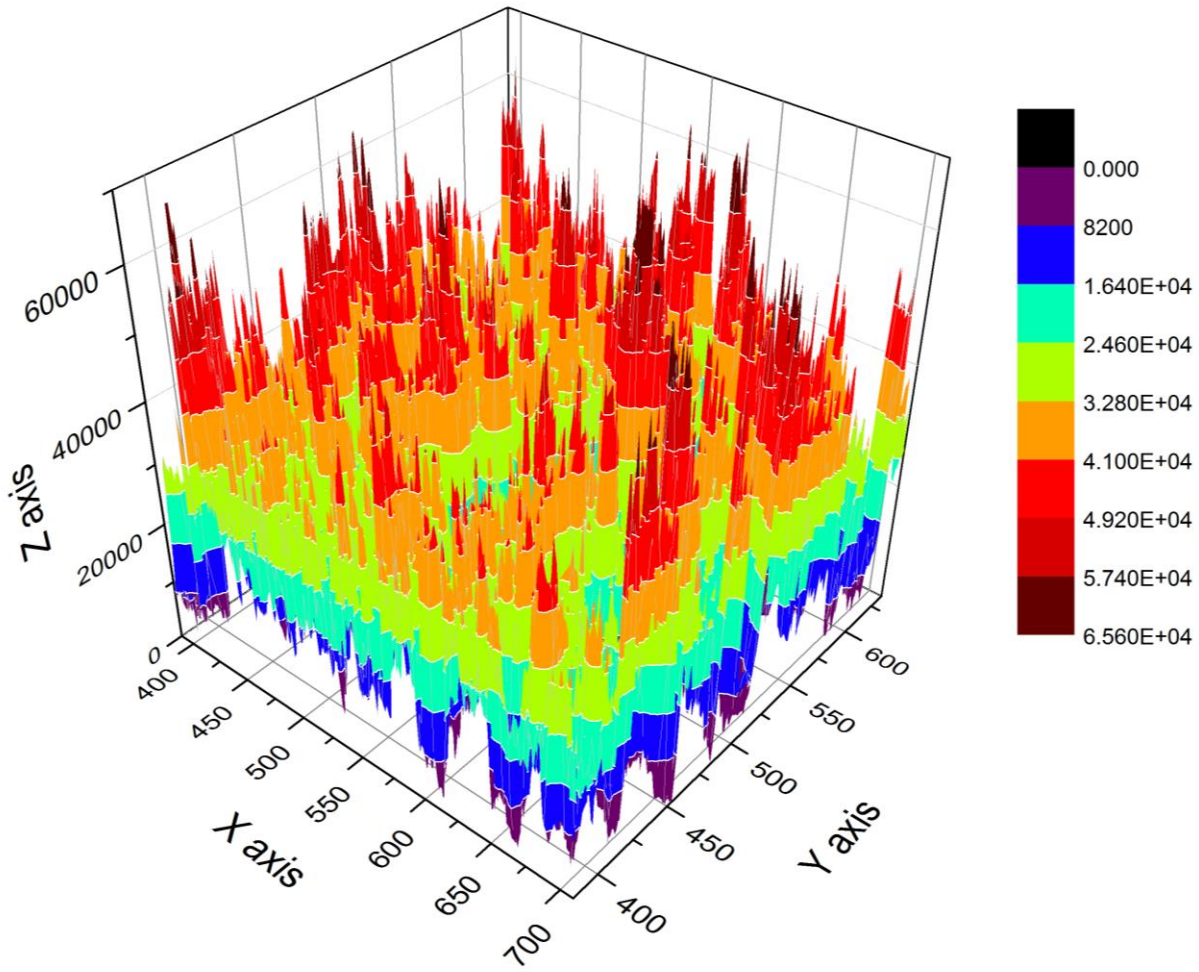

(b)

Figure 3. **(a)** Rebuilt 3D surface of raw rice husk; **(b)** RH-Mn on OriginLab software based on SEM images.

Raw rice husk and RH-Mn were also studied using energy-dispersive X-ray spectroscopy (EDX). In which, Figure 4a presents major components including carbon, oxygen, and silic that could be detected in the raw rice husk. Figure 4b revealed that oxygen concentration was noticeably higher and that the RH-Mn sample contained Mn. As a result, the RH-Mn sample had been grafted with a sizable quantity of manganese oxide. It was discovered that excellent study conditions invariably result in outstanding adsorption capacity. The removal of silicon dioxide by the solvents during the manufacture of RH-Mn, on the other hand, resulted in a reduction in the quantity of silica present. The surface of the raw rice husk was likewise depicted in Figure 4 to be rather flat. RH-Mn surface meanwhile grew thick and uneven. RH-Mn has more surface area since it is bulky and has a rough surface. The contact area between the adsorbent and the sorbents increases as a result.

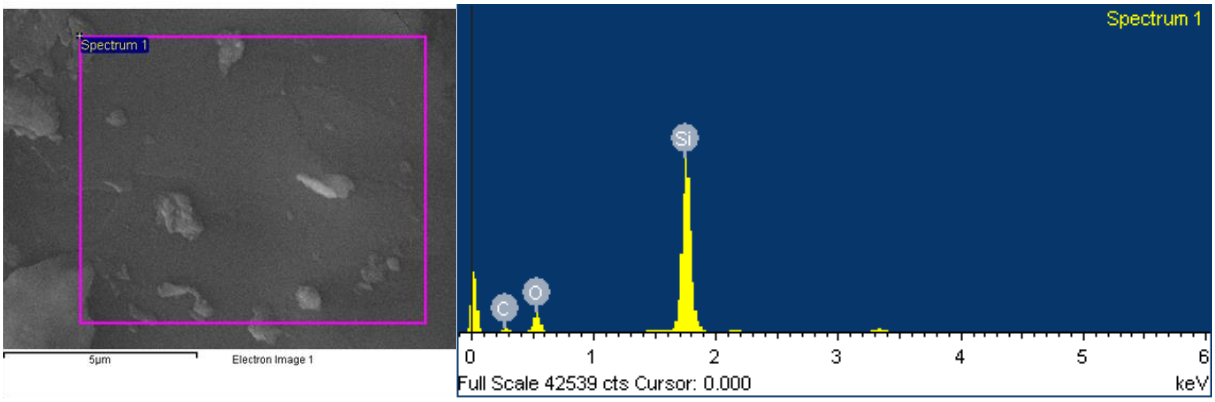

(a)

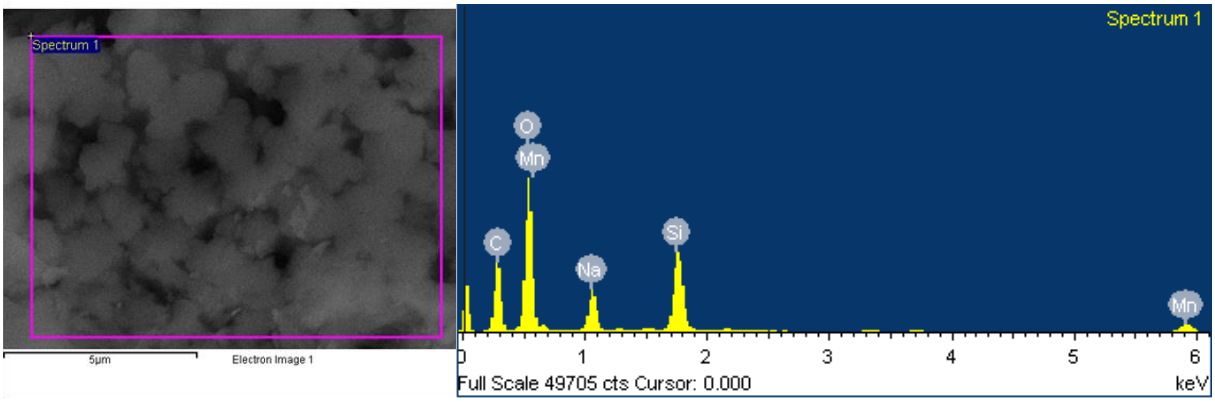

(b)

Note: the axis unit is energy (keV); Y-axis unit is counts

Figure 4. **(a)** EDX spectrum of rice husk and **(b)** manganese oxide coated rice husk (RH-Mn).

3.3. Batch and Adsorption Study

3.3.1. Effect of Contact Time on Adsorption

Figure 5 provides an illustration of how contact time affected the lead ions' ability to bind to RH-Mn. The graph indicating lead uptake removal versus time shows a two-step method. The initial part of the piece shows that the fast adsorption took place in the first 1 to 4 hours. In this study, we did not perform the lead ion removal from the starting point to 1 hour. Because, during this time, the adsorption capacity was unstable and unclear the removal trend. It could be explained by MnO_2 coating area on the surface is not uniform between locations, so the contact between metal ions and the surface is also not uniform. This leads to an unstable adsorption capacity during the compartment period. Therefore, the study presents the adsorption trend at time intervals greater than 1 hour. After that, we observed the equilibrium was only gradually reached after that. Within 4 hours, the bulk of the lead removal was finished.

It took 6 to 8 hours for lead ions to be fully absorbed, and longer response times did not show any discernible differences. Lead ions required time to move from the medium to the material's surface during the initial stage of adsorption. The adsorption capacity in the first step increased significantly as a result. Following that, lead ions filled nearly all of the adsorption locations. Because the lead ion was in competition with one another for adsorption sites. This causes a gradual increase in adsorption capacity throughout the subsequent (6–8 h) time period and slowly reached the equilibrium status. Since equilibrium time might last for around 3 to 4 hours, the application time will be as short as possible.

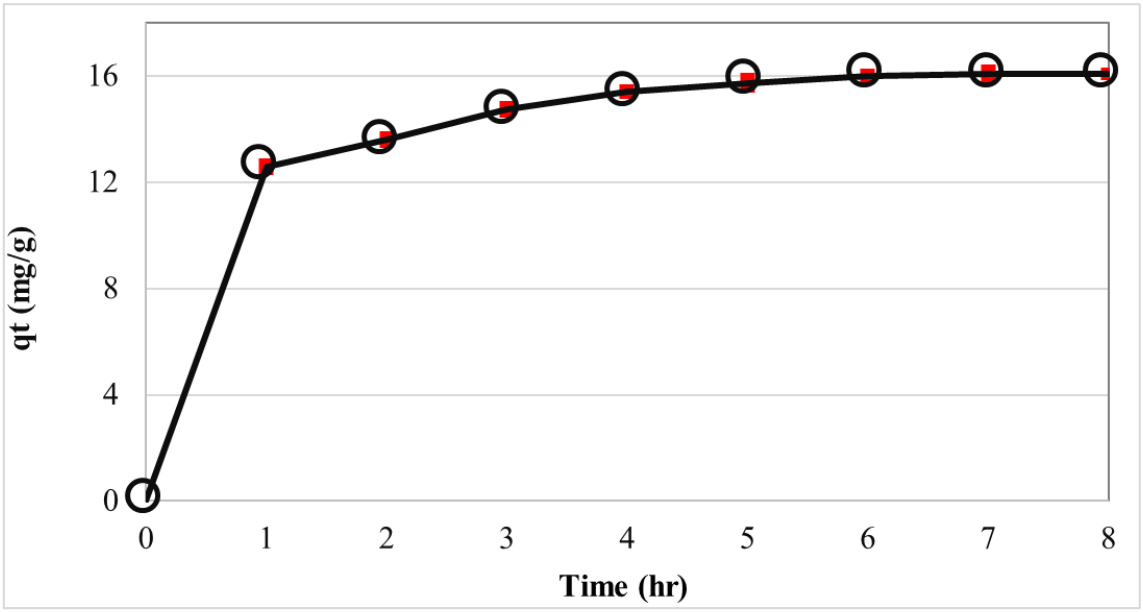

Figure 5. Effect of contact time on removal Lead ions by RH-Mn (conditions: initial Pb(II) concentration was 20 mg/L; RH-Mn concentration dosage was 1g/L; pH was neutral; contact time was set from 1 to 8 hours; stirred 120 rpm; room temperature)

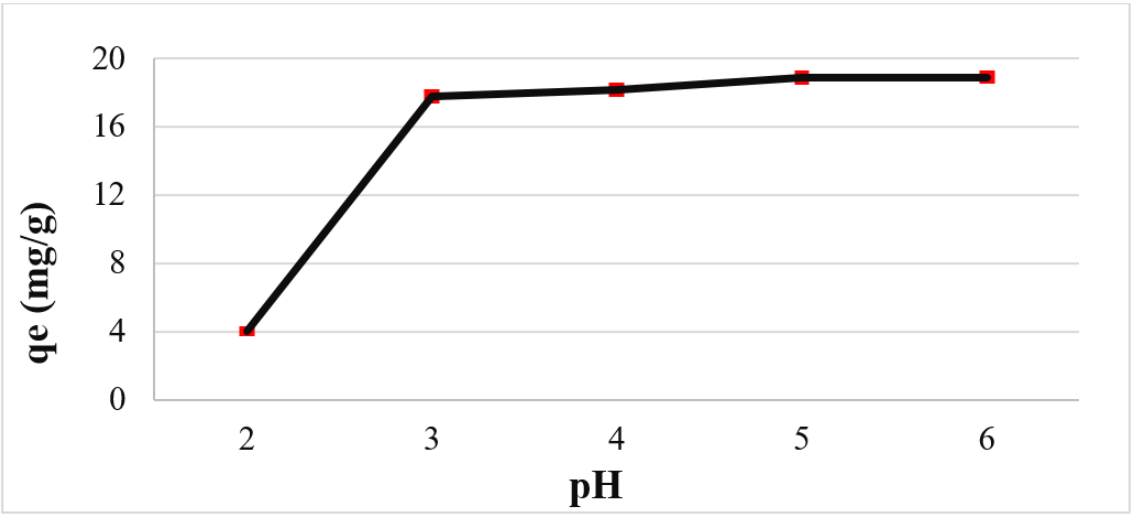

Figure 6. Effect of pH on Lead ions removal by RH-Mn (conditions: pH from 2 to 6; 20 mg/L Pb(II) concentration; RH-Mn concentration was 1 g/L; stirred 120 rpm; room temperature)

3.3.2. Effect of PH on Adsorption by RH-Mn

pH is a critical parameter in the metal adsorption system. It influences the activity of the functional groups on the RH-Mn surface as well as the competition of lead ions for active sites on the adsorbent surface. Under our investigations from relevant studies, the lead ion is precipitated when pH is better than 6. Since we didn't conduct any tests with a pH greater than 6 during the investigation. Because of the precipitation event in the solution between Pb(II) and OH-. Because it impacts both the adsorbent surface and the solution, the initial pH value has a significant impact on how well metal ions are able to bind to surfaces.

pH 6 and pH 2.00 yielded the highest and lowest lead removal rates, respectively. A higher pH than 2, resulted in a higher proportion of lead elimination. This finding might be interpreted by the fight for the adsorbent surface of RH-Mn between lead ions and H_3O^+ ions. The surface was presumably covered with H_3O^+ ions, which accounts for the lower percentage of lead removal at lower pH levels when the number of H_3O^+ ions was many times greater than that of lead ions. The sites for lead ions became accessible as the pH rose because more H_3O^+ ions were converted to H_2O and exited the adsorbent surface.

3.3.3. Effect of Concentration Dosage on Adsorption

The picture of the effect of RH-Mn concentration dosage on Pb(II) removal was drawn under Figure 7. The result

indicated that increasing the adsorbent dose led to decreased adsorbent uptake on lead (Figure 7). This can be attributed to the fact that as the amount of adsorbent is increased, the total surface area available for lead ion adsorption decreases due to overlap or aggregation of adsorption sites [43, 44]. However, it was necessary to evaluate the combination of two factors: the adsorption efficiency and removal efficiency. Because it was related to the economy and cleaning capacity of the adsorbent. Figure 7 also indicates that the removal efficiency increases as the adsorbent dose increases. The results found that using the adsorbent dosage of 1g/L is the most economical and effective.

3.4. Adsorption Study

3.4.1. Kinetic Study

As a function of the amount of time that a liquid and solid are in contact, kinetic research indicates how much adsorption capacity is consumed. By examining the Pb(II) ion adsorption from aqueous solutions at various time intervals (1–8 hours), while maintaining the other variables constant, the adsorption kinetics was discovered. The equations in Table 1 show the use of the pseudo-first-order and second-order models to comprehend the mechanism for the adsorption process. The correlation coefficient values (R^2) for the experimental data were greater than 0.95, as shown in Table 1, and both models matched the data well (Figure 8). In contrast to the Pseudo-first order (0.9647) kinetic model, a greater correlation coefficient (R^2) value was found from the Pseudo-second order (0.9996). The adsorption may have followed the pseudo-second-order kinetics more closely, according to this. As a result, lead ion adsorption by producing MnO_2 on rice husk with nanostructures is expected, which is regulated kinetically as a second-order reaction rather than a first-order one. The quadratic model presupposes rate-limiting procedures for the chemical changes. The outcomes also suggest that the adsorbent is good and has great potential for removing lead ions from aqueous solutions with a range of concentrations.

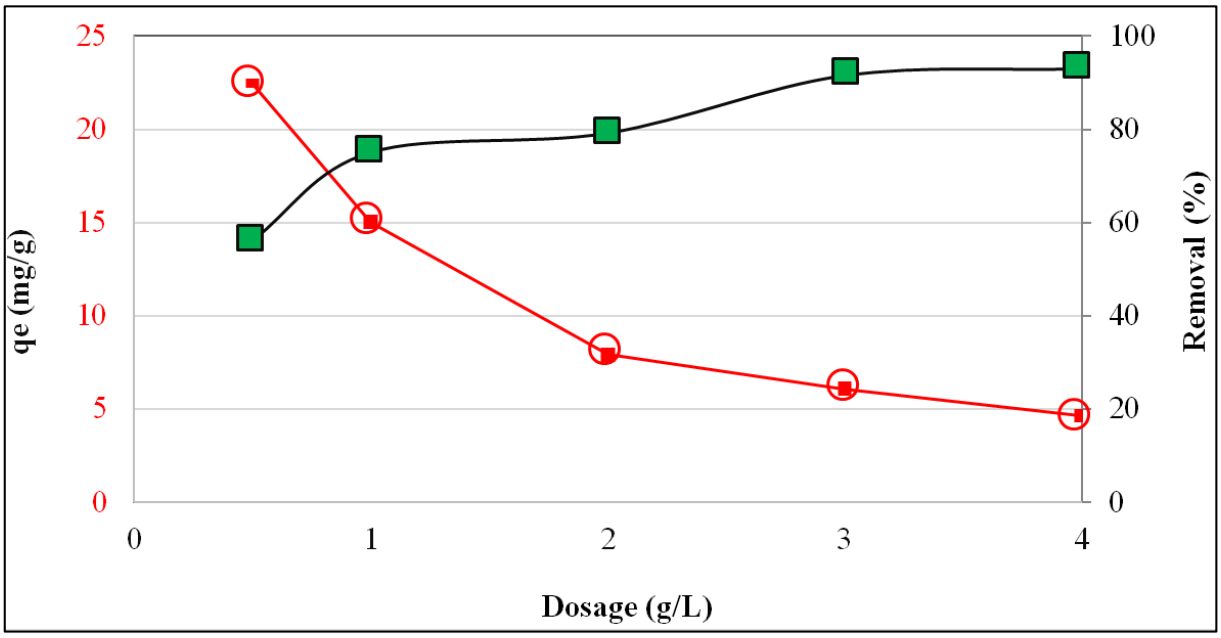

Figure 7. Effect of adsorbent dosage on lead uptake (conditions: RH-Mn dosage from 0.5 to 4 g/L; initial Pb(II) concentration was 20 mg/L; time contact was 4 hours; room temperature; stirred 120 rpm; pH was 4)

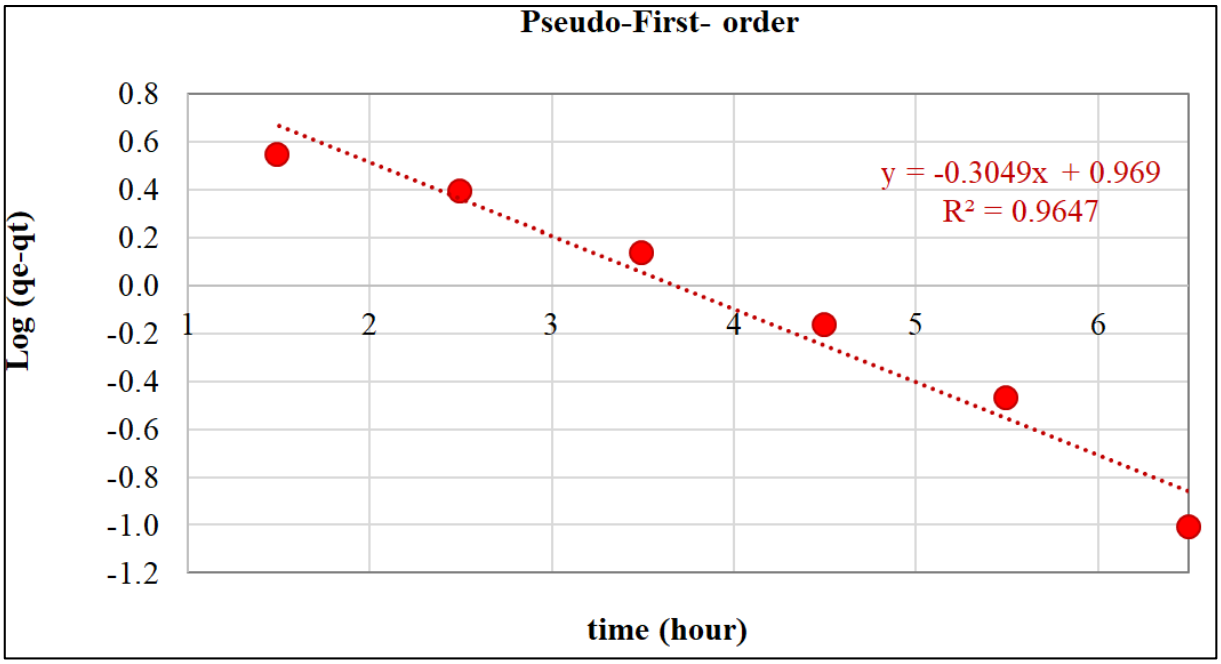

a)

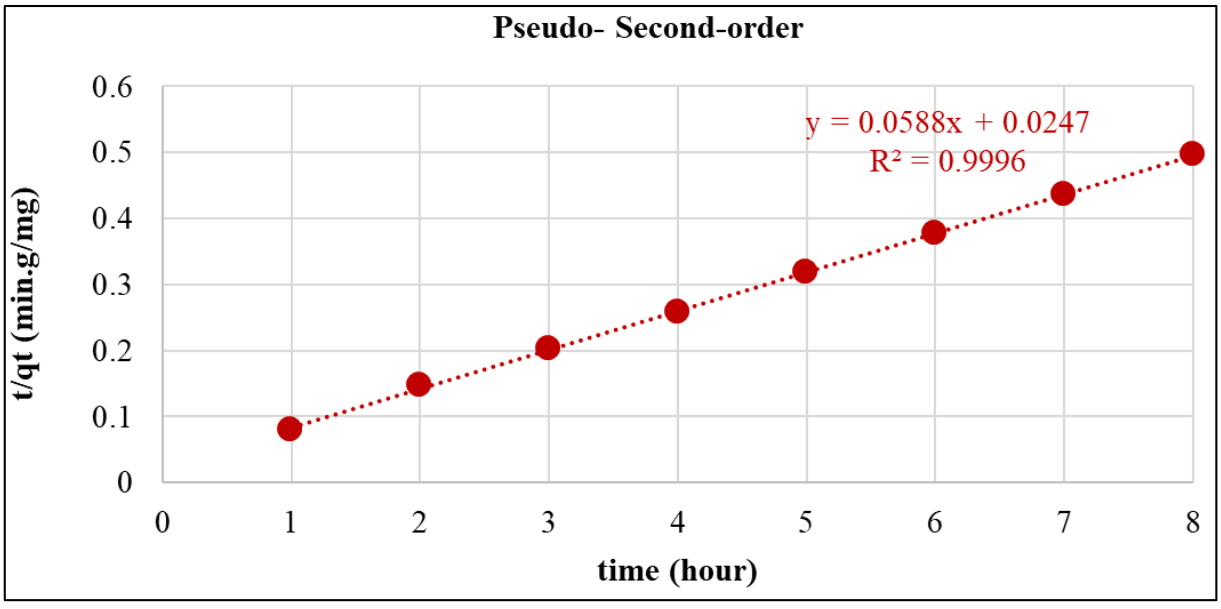

b)

Figure 8. **(a)** Pseudo-first (Log (qe – q_t) vs. time) and **(b)** Pseudo-second orders model for removal Lead ions adsorption by RH-Mn (t/q_t vs. time).

Table 1. Kinetic model: Pseudo-first and Pseudo-second constants.

Pseudo first constants			**Pseudo second constants**		
q_e $(\frac{mg}{a})$	K_1 (h^{-1})	R^2	q_e $(\frac{mg}{a})$	K_2 (g/mg.h)	R^2
9.311	0.702	0.9647	17	0.14	0.9996
The experimental values					
q_e (mg/g) 75.75					

3.4.2. Isotherm Study

The isotherm models include Langmuir, Freundlich, Temkin, and D-R models are shown in Figure 9. The high R^2 was obtained by fitting experimental data into the Freun-dlich with correlation coefficient value is the highest (R^2 > 0.99945), following the Temkin isothermal model (R^2 > 0.98), compared to the D-R isothermal model (R^2 > 0.97), and the Langmuir's R^2 is over 0.9399 (Table 2). Freundlich's model indicates that the adsorption occurred significantly on the heterogeneous surface by physical adsorption because n >1 (Table 2), the adsorption is favorably a physical process. The manganese oxide often has a negative charge [35]. It reacts with a positive charge from lead ions species that are associated with either positive or neutral charge [36]. The Langmuir model was less satisfied with the study compared with other models. However, it could be considered with the R^2 value. Hence, the adsorption capacity achieved from the Langmuir model was over 73.53 mg/g, and $R_L=1/(1+K_LC_0)$ =0.5. The value is the range between 0 and 1 it denotes that the adsorption is also favorable [37].

For Temkin model was plotted between q_e and L_nC_e (Figure 9c), and its parameters were estimated: K_t = 1.12 (L/mg), bt = 257.43 (kJ/mol), and R^2 = 0.988. It indicates that electrostatic interaction has occurred in adsorption [11, 38]. The constant bt is related to the heat of adsorption in the Temkin model. Its value was positive - indicating an exothermic process [14]. D-R isotherm model was also satisfied with the correlation coefficient (R^2) is 0.9702. In addition, the sorption free energy E (kJ/mol) is computed by the following equation: $E = (2K_{ad})^{-1/2}$ [39], E value is 0.77 kJ/mol, its value is less than 8 kJ/mol. It denotes that the adsorption process was physisorption [11].

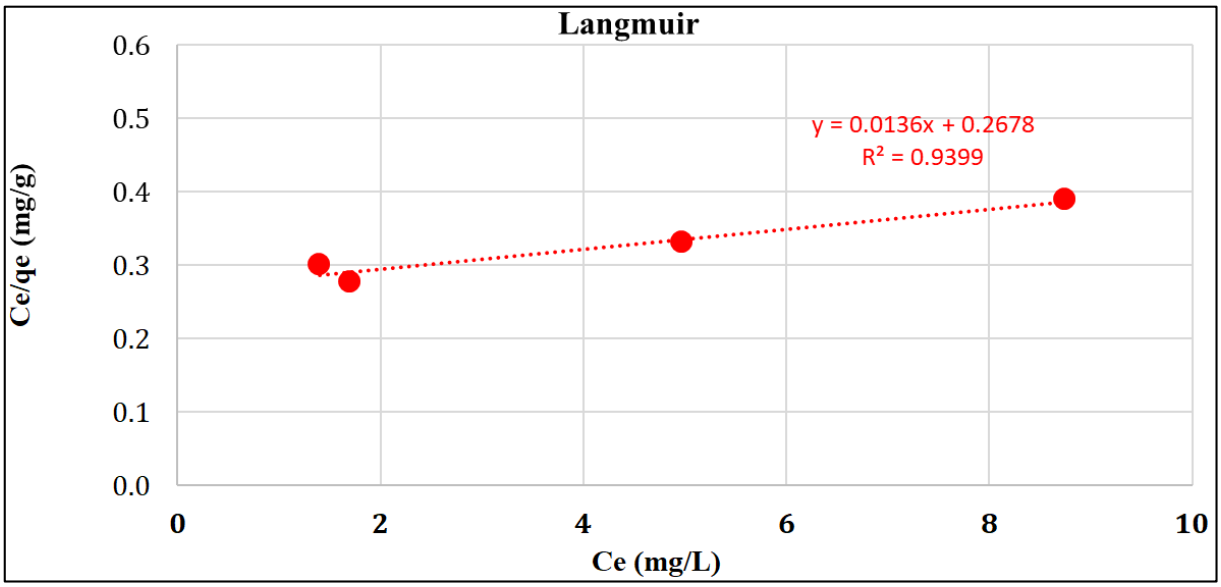

a)

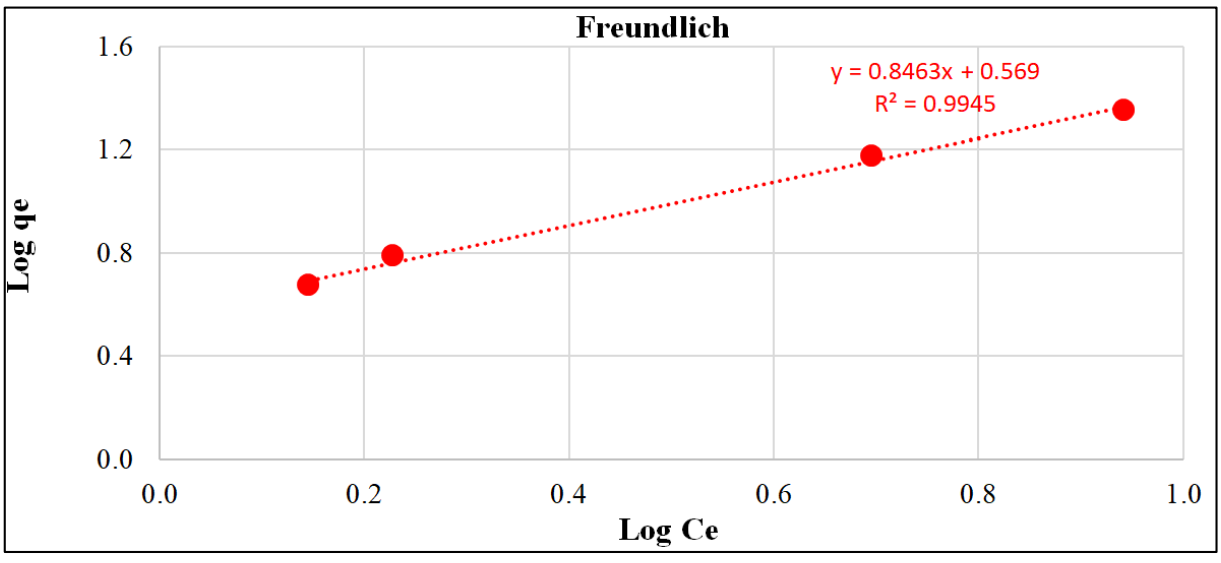

b)

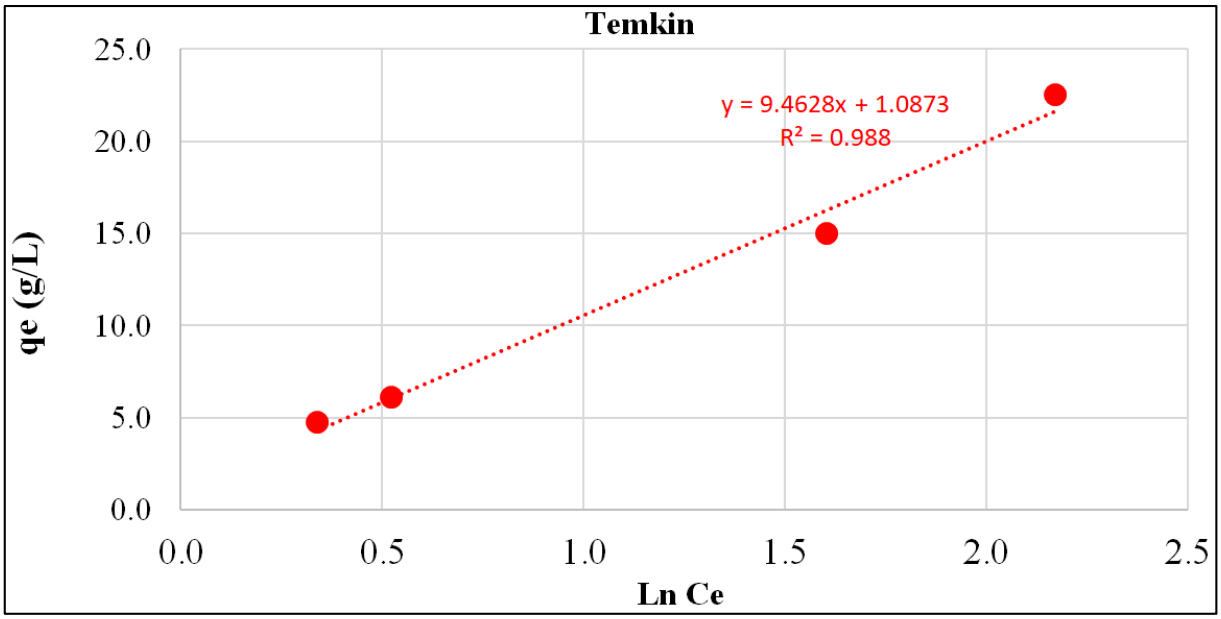

c)

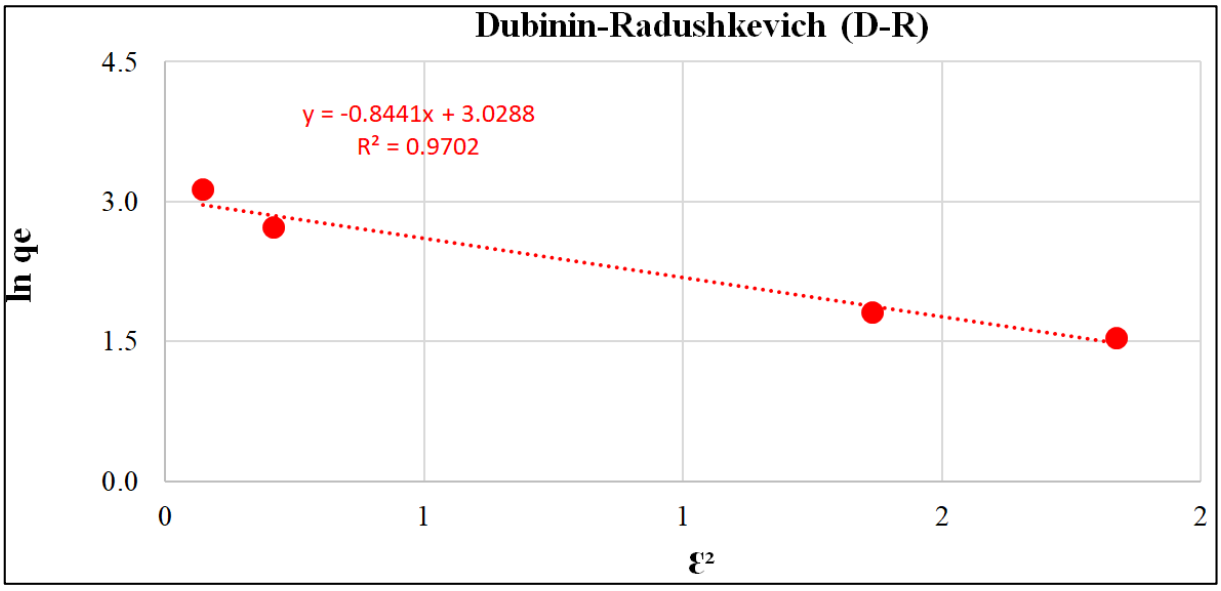

d)

Figure 9. Adsorption isotherm models: **(a)** Langmuir; **(b)** Freundlich; **(c)** Temkin; **(d)** D-R.

Table 2. Langmuir, Freudlich, Temkin, and D-R parameters for Lead ions adsorption by RH-Mn.

Langmuir constants				**Langmuir constants**		
q_{max} (mg/g)	b (L/mg)	R_L	R^2	K_f (mg/g)(L/mg)$^{1/n}$	n	R^2
75.53	0.05	0.5	0.9399	1.18	3.71	0.9945
Temkin constants				**D-R constants**		
K_t (L/mg)		bt (J/mol)	R^2	K_{ad} (mol^2/kJ^2)	q_s	R^2
1.12		257.43	0.988	0.84	20.67	0.9702

Adsorption capacity can be given in three phases in general: (1) In the first stage, lead ions move through the solution and approach the adsorbent surface. (2) In the second step, surface diffusion is mentioned - lead ions move from the top of the surface liquid boundary and transit among nearby adsorption sites on the surface. (3) Diffusion model - lead ions to trap within wholes, resulting in the equilibrium phenomena.

3.5. Adsorption Optimization Study by Response Surface Methodology

Analysis of Variance (ANOVA) is a statistical analysis method that divides aggregate variability within a data set into two parts: systematic components and random factors [27]. The presented data set is statistically affected by the systematic factors but not only the random factors [28, 29]. In regression, research analysts employ the ANOVA test to examine the impacts of independent factors on the dependent variable. The ANOVA test allows for the simultaneous analysis of more than two groups to see whether there is a link between them. The F-statistic (F-ratio), which is a byproduct of the ANOVA formula, enables the study of numerous sets of data to ascertain the variability within and across samples [29, 30]. In a regression model, R^2 (also known as R^2 or the coefficient of determination) is a statistical metric that quantifies how much of the variation in the dependent variable can be accounted for by the independent variable. Thus, R^2 displays the degree to which the data are consistent with the regression model (the goodness of fit). The index is between 0 and 1. All values between 0 and 1 are acceptable for R^2. Even though the statistical measure offers some insightful information about the regression model, the user shouldn't solely depend on the measure when evaluating a statistical model. The graph does not reveal anything about the causal link between the variables that are both independent and dependent. Besides, the formula for calculating R^2 can be expressed as [31-32]:

$$R^2 = \frac{SS_{regression}}{SS_{total}}$$

Where:

$SS_{regression}$: Resulting from regression, it is the sum of squares (explained sum of squares)

SS_{total}: which is the sum of all squares

Moreover, it does not illustrate the accuracy of the linear regression. As a result, when studying r-squared in conjunction with the other variables in a statistical model, the researcher should indeed make inferences about the model.

The statistical analysis using ANOVA for a quadratic model connected to four driving elements including pH, contact duration, beginning concentration of lead ions, and concentration dose was examined (Table 4 and Table 5)… These components were provided and assigned names A, B, C, and D, respectively, in the model. For the optimization procedure, five levels for each variable were defined to analyze the effect of its amounts on adsorption removal (unit: %). Each element in the Central Composition Design was coded in the range (-1, +1) - representing the low (-1) and high level (+1) [31, 32]. The axial points are located at a distance α from the center, making the design rotatable and fixed at level 2. Centralized test copies are useful because they give independent estimates of test errors as well as data run repeatability [23, 25]. In the middle, the planned number of experiments for the four variables is six. As a result, the number of test runs (N) is examined in the following manner.

$$N = 2^2 + 2n + n_c = 2^4 + 2 + 6 = 30$$

Furthermore, the range and levels of the parameters for each variable were shown in Table 3.

Table 3. Experimental range and levels for each variable for RH-Mn adsorption.

Variables	-α	-1	0	+1	α
pH	2	3	4	5	6
Contact time	1	2	3	4	5
Pb(II) concentration	0	5	10	15	20
Dose adsorbent	0.5	1	1.5	2	2.5

According to the results in Table 4, certain crucial factors from the data, such as the Fisher value (F-value) (136.9), suggest that the model is significant, and p-values less than 0.05 shows that model terms are significant [28]. Furthermore, the coefficient of determination (R^2) value was high in the study (0.9922). It signifies that the model can explain both the experimental and projected data. Further, adjusted R^2 = 0.9850 was acceptable, showing the model's relevance. Furthermore, the appropriate precision rating of 39.7621 suggests that the signal is adequate [17]. Moreover, the coefficients for the linear influence of chosen parameters such as (A) pH, (B) Time, (C) Pb(II) concentration, and (D) adsorbent dosage were less than 0.05 for every probability (p-value), denoting that they are highly important in the outcome. Furthermore, the coefficient values for the quadratic impacts of A^2 (pH), B^2 (Time), and D^2 (adsorbent dosage) are less than 0.05 for all p-values, indicating that they are significant factors. Likewise, the correlations AB; AD; BC; BD; and CD are crucial for this model (Table 4). Meanwhile, C^2 (Immediate Pb(II) concentration) and AC are minor.

Table 4. The regression coefficients (ANOVA) of the adsorption efficiency by RH-Mn.

Variables	Sum of Squares	df	Mean Square	F-value	p-value	
Model	1317.64.89	14	94.12	136.9	< 0.0001	Significant
A-pH	336.76	1	336.76	489.84	< 0.0001	Significant
B-Time	394.64	1	394.64	574.07	< 0.0001	Significant
C-Pb(II) concentration	13.57	1	13.57	19.74	< 0.0005	Significant
D-Dose adsorbent	136.01	1	136.01	197.83	< 0.0001	Significant
AB	19.58	1	19.58	28.49	< 0.0001	Significant
AC	0.2551	1	0.2551	0.3711	0.5515	Insignificant
AD	6.61	1	6.61	9.62	0.0073	Significant
BC	4.60	1	4.60	6.60	0.0206	Significant
BD	9.31	1	9.31	13.55	0.0022	Significant
CD	5.72	1	5.72	8.32	0.0113	Significant
A^2	113.42	1	113.42	164.98	<0.0001	Significant
B^2	226.28	1	226.28	329.14	<0.0001	Significant
C^2	2.12	1	2.12	3.09	0.0991	Insignificant
D^2	115.24	1	115.24	167.62	< 0.0001	Significant
Residual	10.31	1	0.6875			
Lack of fit	7.2	10	0.724	1.16	0.4623	
Pure error	3.11	5	0.6217			
Cor total	1327.95	29				
Standard deviation	**Mean**	**C.V%**	**R^2**	**Adjusted R^2**	**Predicted R^2**	**Adequate precision**
0.8291	91.26	0.9085	0.9922	0.9850	0.9654	39.7621

Table Central composition Design matrix for the Design Expert Software 11 with the actual and predicted values for recommended 30 tests are shown in Table 5 Central Composition Design (CCD) has been applied to develop polynomial regression equations, all of which are quadratic expressions proposed by the software [18]. Theoretically, the mathematical relationship between the four independent elements can be approximated by a quadratic polynomial model (Equation (1*)) [19].

$$X = b_0 + b_1x_1 + b_2x_2 + b_3x_3 + b_4x_4 + b_{12}x_1x_2 + b_{13}x_1x_3 + b_{14}x_1x_4 + b_{23}x_2x_3 + b_{34}x_3x_4 + b_{11}x_1^2 + b_{22}x_2^2 + b_{33}x_3^2 + b_{44}x_4^2 \quad (1^*)$$

Where, X is a response for removal efficiency (%), b_0 is constant, b_1, b_2, b_3, and b_4 are linear coefficient, b_{12}, b_{13}, b_{14}, b_{23}, and b_{34} are cross-product coefficients, b_{11}, b_{22}, b_{33}, and b_{44} are quadratic coefficients; A (pH), B (Time), C (Initial Pb(II) concentration), and D (Dosage concentration). For the study, the model expression has been chosen according to the total sequential model based on the highest order of polynomials in which the model is not aliased and additional terms make sense [20]. The coded equation can be presented as the following equation below (2*):

$$\text{Removal (Percentage)} = 96.6 + 3.75A + 4.06B + 0.752C + 2.38D + 1.11AB - 0.1263AC - 0.6429AD - 0.5363BC - 0.598CD - 2.3A^2 - 2.287B^2 + 0.2783C^2 - 2.05D^2 \quad (2^*)$$

The actual equation is shown by the equation below (3):

$$\text{Removal (percentage)} = -24.03292 + 18.876A + 20.224B + 0.7093C + 41.471D + 1.106AB - 0.0252AC - 1.2858AD - 0.10725BC - 1.52589BD - 0.2392DC - 2.3349A^2 - 2.87224B^2 + 0.01113C^2 - 9.19889D^2 \quad (3^*)$$

Table 5. Response (Removal, unit %) data of adsorption of RH-Mn based on experimental design matrix.

Order	Factors				Response removal (%)	
	pH	Time (h)	Initial Pb(II) concentration	Dose absorbent (g/L)	Actual	Predicted
1	5	2	5	1	83.73	84.25
2	5	4	5	2	98.94	100
3	2	3	10	1.5	80.51	80.97
4	5	4	15	2	99.45	99.29
5	4	3	10	1.5	98.21	96.60
6	6	3	10	1.5	96.43	95.96
7	4	3	10	1.5	96.31	96.6
8	3	2	5	1	77.57	77.43
9	4	3	0	1.5	97.23	96.21
10	4	3	10	1.5	96.22	96.6
11	4	3	10	1.5	96.27	96.6
12	4	3	10	0.5	83.27	83.64
13	5	2	15	1	87.9	87.77
14	3	2	15	1	82.54	81.46
15	5	2	15	2	91.79	91.58
16	5	2	5	2	90.6	90.45
17	3	4	5	2	91.8	91.65
18	3	2	5	2	85.87	86.2
19	4	3	10	1.5	96.25	96.6
20	3	4	15	1	87.94	87.81
21	4	3	10	2.5	93.55	93.17
22	4	3	20	1.5	98.21	99.22
23	3	2	15	2	87.88	87.83
24	4	3	10	1.5	96.36	96.6
25	4	1	10	1.5	76.54	77
26	3	4	5	1	85.42	85.93
27	3	4	15	2	91.35	91.13
28	5	4	5	1	97.41	97.17
29	4	5	10	1.5	93.7	93.22
30	5	4	15	1	98.59	98.55

Figure 10a depicts a plot of the expected and actual value of the removal (%) from the design model, with the adjusted and predicted R^2 being near, indicating good agreement with the model. The perturbation plot (shown in Figure 10b) allows you to compare the impacts of all elements at a single location in the design space. Feedback is generated by modifying only one element within its scope while leaving all other elements intact. By default, Design-Expert sets the reference point in the center (coded 0) of all components. [21].

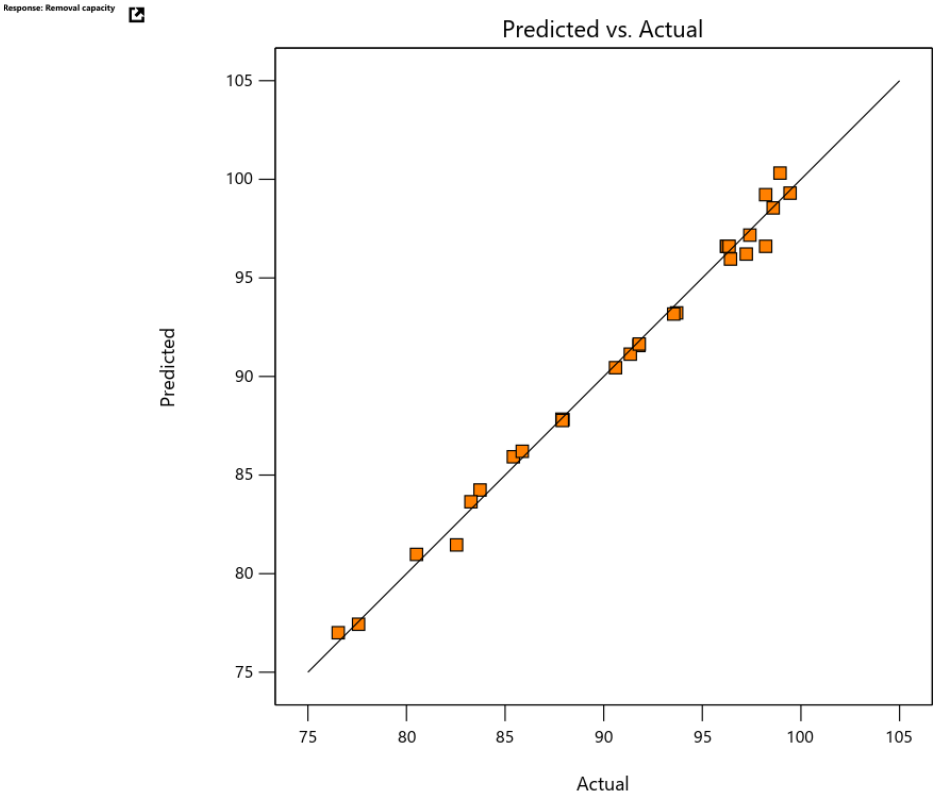

(a)

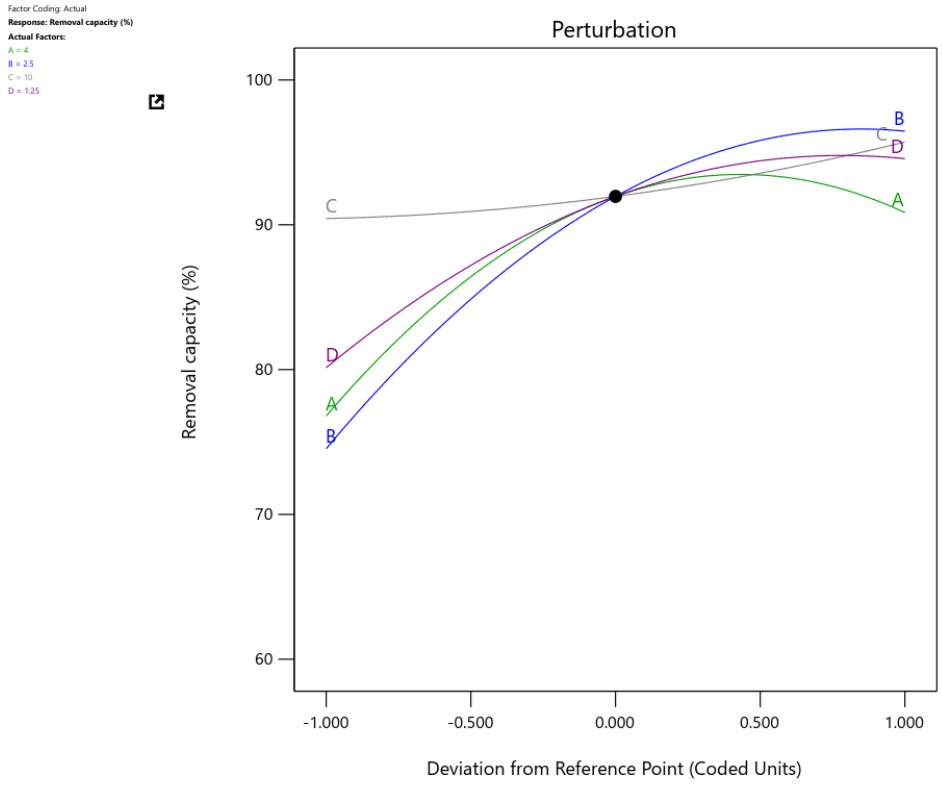

(b)

Figure 10. **(a)** Actual results versus predicted results of the model; **(b)** perturbation plot.

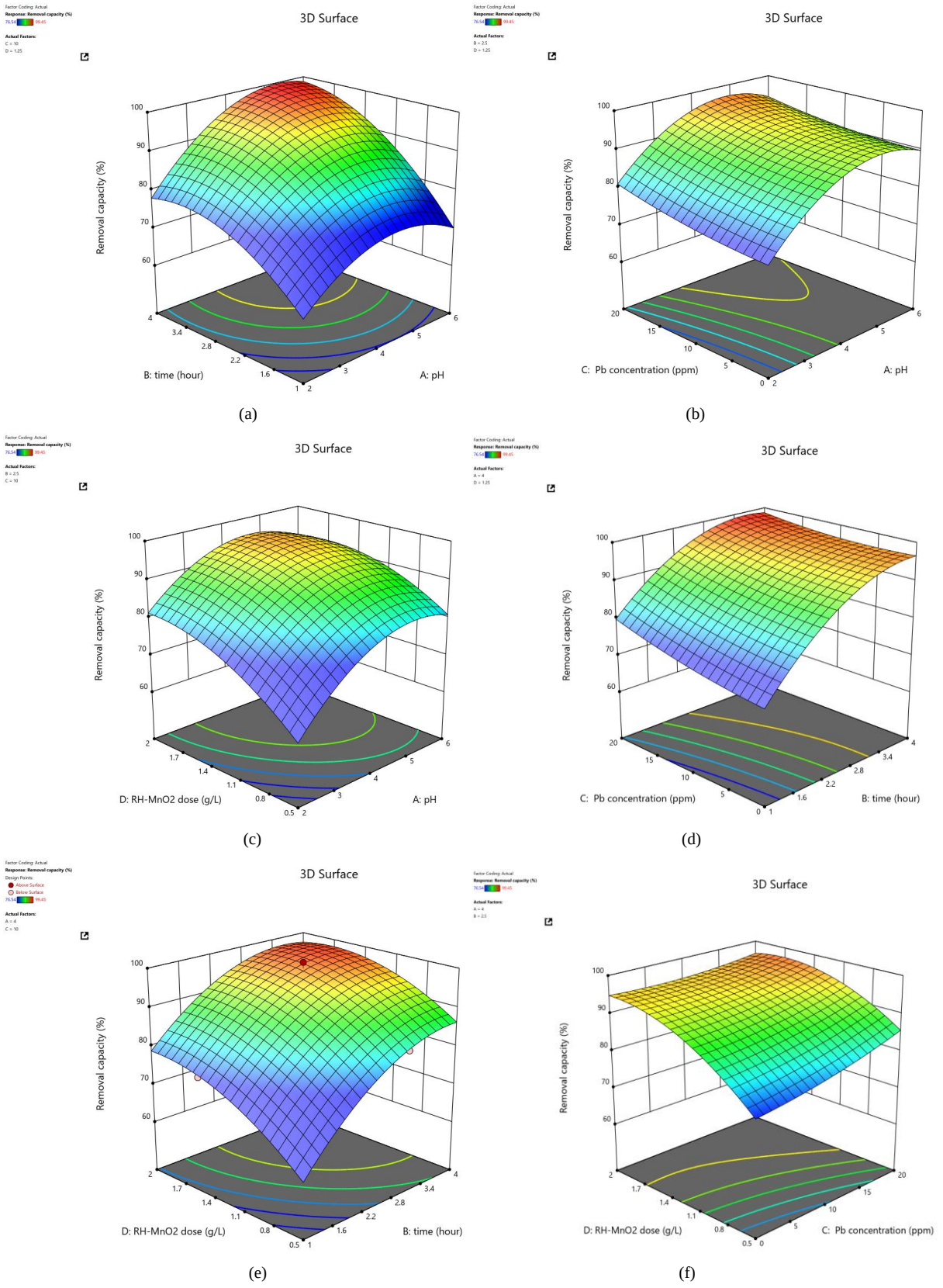

Figure 11. Response surfaces plot. **(a)** Interaction plot time and pH, **(b)** plot between initial Pb(II) concentration and pH, **(c)** plot of pH and dose concentration **(d)** Plot of initial concentration Pb(II) and time, **(e)** plot of time and dose concentration, and **(f)** plot of dose concentration and initial Pb(II) concentration.

Figure 11 depicts the interaction of four factors with lead ion removal (Unit: %) using three-dimensional response surface plots. Figure 11a shows that the trend of increasing time and pH resulted in a quick rise in Pb(II) elimination, with the ideal pH estimated to be about 4. Figure 11b depicts the plotted relationship between Pb(II) concentration and pH, with a pH range of roughly 4 achieving the vast majority of removal. Figure 11c shows that increasing the quantity of adsorbent from 0.5 to 2 leads to increased removal (%). However, at higher concentration dose, percentage removal appears to be maintained and slightly decreased. It may be explained by the fact that aggregation adsorbent particles overlapped, reducing the availability of exchangeable sites for the ions in the adsorbent [22]. Figure 11d shows that as contact duration grows, adsorption removal increases because the active sites of the adsorbent and Pb(II) molecules need to catch and interact. Figures 11e and 11f demonstrated that an appropriate dose concentration and time of 1.5g/L and 3 hours could be adequately accomplished for the research.

This study also provided the adsorption capacity of lead ions by several composite materials compared with our adsorbent (Table 6). It indicates that rice husk is modified by manganese oxide which can be a potential adsorbent. Although its adsorption capacity does not be outstanding, however, it completely eliminates lead ions from an aqueous solution that is a highlight of this study.

4. Conclusions

The adsorption of lead ions on rice husk modified manganese oxide an (RH-Mn) from acidic aqueous solution was investigated in this study and the following conclusions can be drawn:

1) The RH-Mn can be synthesized by depositing manganese oxide on rice husk from the potassium permanganate solution.
2) The adsorption removal significantly increased with the increase in pH from 2-4.
3) The kinetic data indicated that lead ion adsorption follows second-order kinetics model with a high correlation coefficient (R^2 =0.9996).
4) The adsorption equilibrium was achieved at four hours and the experimental adsorption capacity of 16 mg/g was observed at pH 4 (lead ion initial concentration of 20 mg/L). The adsorption equilibrium was explained by Freundlich and Dubinin-Radushkevich models representing multilayer adsorption.
5) The experimental design, response surface methodology (RSM), was applied to optimize the lead ion adsorption onto RH-Mn.
6) Over 99% of lead ions were removed at optimized conditions: contact time; 3 hours, pH; 4, initial lead ion concentration; 15 mg/L, and RH-Mn dosage.

Therefore, it can be concluded that RH-Mn can be used to remove lead ions from water.

Table 6. Comparison of adsorption capacity - lead ions removal by some adsorbents.

Materials	pH	q_e (mg/g)	Ref.
Polypyrrrole-based activated carbon	5.5	50	4
Peanut hull ash	4.3	68.5	11
Moringa oleifera bark	5	34.6	35
Tea waste	5-6	65.5	31
Activated carbon from precursor hazelnut husks	5.7	13.05	40
Chitosan/cellulose composite	5.3	27.31	41
Chitosan – polymerizing methacrylic nanoparticle (CS-MAA)	5	11.3	42
ZnO/talc nanocomposite	4	48.3	43
Crosslinked chitosan-clay beads	6	34.13	44
ZnO/MMT (minerals montmorillonite) nanocomposites	6	88.5	45
Rice husk modified by manganese oxides	4	75.53	This study

Supplementary Materials:

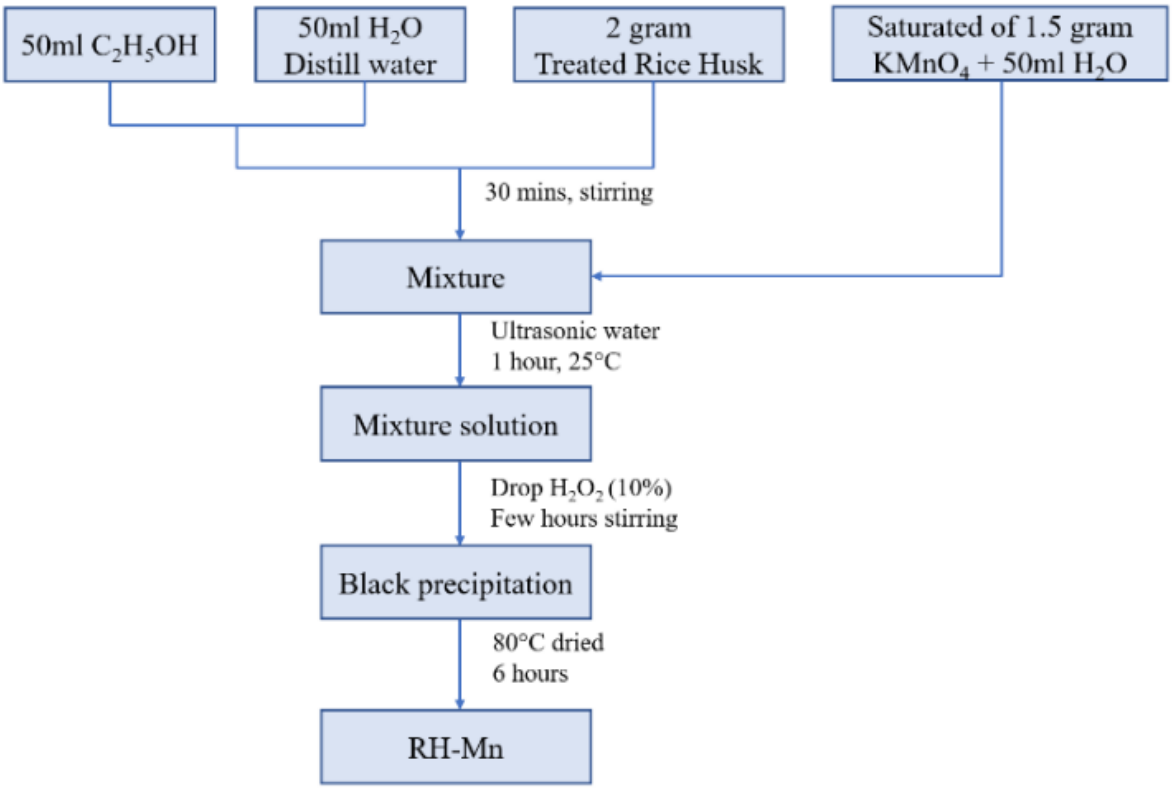

Figure 1. The process of synthesis of rice husk MnO_2.

REFERENCES

[1] R. Zhang, Wilson, V. Wilson, A. Hou, G. Meng. Source of lead pollution, its influence on public, 18–31, 2015. http://dx.doi.org/10.13130/2283-3927/4785.

[2] H. Zhang, A. Wu, H., Fu, L. Zhang, H. Liu, S. Zheng, H. Wan, Z. Xu. Efficient removal of Pb (II) ions using manganese oxides: The role of crystal structure. RSC Advances, 7, 41228–41240, 2017. doi:10.1039/c7ra05955h.

[3] D. Kundu, S. Mondal, D. Dutta, S. Haque, A. R. Ghosh. Accumulation, and contamination of lead in different trophic levels of food Accumulation and contamination of lead in different trophic levels of food chain in sewage-fed East Kolkata Wetland, West Bengal, India. International Journal of Environmental Technology Science, 2, 61-68, 2016.

[4] A. A. Alghamdi, A. B. A. Odayni, W. S. Saeed, A. A. Kahtani, A. A. Alharthi, T. Aouak. Efficient Adsorption of Lead (II) from Aqueous Phase Solutions Using Polypyrrole-Based Activated Carbon, Materials (Basel, Switzerland), 2019. doi: 10.3390/ma12122020.

[5] C. Fenga, S. Gangemi, V. D. Salvatore, L. Falzone, M. Libra. Immunological effects of occupational exposure to lead (Review), Molecular Medicine Report, 3355–3360, 2017. doi: 10.3892/mmr.2017.6381.

[6] H. C. Kim, T. Jang, H. J. Chae, W. J. Choi. Evaluation and management of lead exposure. Annals of Occupational and Environmental Medicine, Vol. 27, No.1, 1-9, 2015. doi: 10.1186/s40557-015-0085-9.

[7] L. H. Mason, J. P. Harp, D. Y. Han. Pb Neurotoxicity: Neuropsychological Effects of Lead Toxicity, BioMed Research International, 2014.

[8] S. K. Gunatilake. Methods of Removing Heavy Metals from Industrial Wastewater, Journal of Multidisciplinary Engineering Science Studies, Vol. 1, No 1, 2015.

[9] H. Chisti. Heavy metal sequestration from contaminated water: A review, Environmental Science, 2508, 2345–2355, 2018.

[10] J. O. Lima, M. F. Ragassi, M. L. Gimenes, M. G. A. Vieira, M. G. C. Da Silva. Equilibrium study of cadmium Ion's adsorption on Sericin/Alginate particles, Chemical Engineering Transactions, 56, 1891–1896, 2017. doi: 10.3303/CET1756316.

[11] S. Mireles, J. Parsons, T. Trad, C-L Cheng, J. Kang. Lead removal from aqueous solutions using biochars derived from corn stover, orange peel, and pistachio shell, International Journal of Environmental Science and Technology, 16, 5817-5826, 2019.

[12] A. S. Ayangbenro, O. O. Babalola. A New Strategy for

Heavy Metal Polluted Environments: A Review of Microbial Biosorbents. Vol 14, No 1, 2017. doi: 10.3390/ijerph14010094.

[13] R. Long, H. Ouyang, H. Guo. Super-slack-based measuring data envelopment analysis on the spatial – temporal patterns of logistics ecological efficiency using global Malmquist Index model. Environmental Technology & Innovation Environ, Vol. 18, No 4, 100770, 2020. doi: 10.1016/j.eti.2020.100770.

[14] F. Moughaoui, A. Ouaket, M. Eddebbagh, A. Bennamara, A. Abdelmjid, Z. Anbaoui, M. Berrada. Study of adsorption isotherms and kinetic models of methylene blue adsorption on moroccan bagasse waste, Conference: 7th International Conference on Innovation in Chemical, Agricutural, Biological abd Environmental Sciences, London, Uk, 2017.

[15] V. C. Srivastava, I. D. Mall, I. M. Mishra. Optimization of parameters for adsorption of metal ions onto rice husk ash using Taguchi's experimental design methodology. Chemical Engineering Journal, Vol. 140, No. 1-3, 136–144, 2008. doi: 10.1016/j.cej.2007.09.030.

[16] H. A. Sani, M. B. Ahmad, M. Z. Hussein, N. A. Ibrahim, A. Musa, T. A. Saleh. Nanocomposite of ZnO with montmorillonite for removal of lead and copper ions from aqueous solutions. Process Safety and Environmental Protection, 10, 97-105, 2017. https://doi.org/10.1016/j.psep.2017.03.024.

[17] M. C. Hoyos-sánchez, A. C. Córdoba-pacheco, L. F. Rodríguez-herrera, R. Uribe-kaffure. Removal of Cd (II) from Aqueous Media by Adsorption onto Chemically and Thermally Treated Rice Husk. Journal of Chemistry, 2017.

[18] A. G. El-Said, N. A. Badway, S. Garamoun. Adsorption of Cadmium (II) and Mercury (II) onto Natural Adsorbent Rice Husk Ash (RHA) from Aqueous Solutions: Study in Single and Binary System, 6, 400–409, 2010.

[19] J. Qi, Y. Li, H. Majeed, H. D. Goff, R. T. Rahman, Llc, F. Zhong. Adsorption mechanism modeling using lead (Pb) sorption data on modified rice bran-insoluble fiber as universal approach to assess other metals toxicity. International Journal of Food Properties, Vol. 22, No. 1, 1397–1410, 2019. doi: 10.1080/10942912.2019.1650764.

[20] M. M. Hammo, T. Akar, F. Sayin, S. Celik, S.T. Akar. Efficacy of green waste-derived biochar for lead removal from aqueous systems: Characterization, equilibrium, kinetic and application. Journal of Environmental Management, 289, 112490, 2021. https://doi.org/10.1016/j.jenvman.2021.112490.

[21] Z. Wihua, J. Zhang, K. Li, P. Han, R. Han. Characterization of Manganese Oxide, and the Adsorption of Copper (II) and Lead (II) Ions from Aqueous Solutions. Adsorption Science & Technology, 549–565, 2009.

[22] B. Kamal, A. Rafey. A mini review of treatment methods for lead removal from wastewater. International Journal of Environmental Analytical Chemistry, 1-16, 2021. https://doi.org/10.1080/03067319.2021.1934833.

[23] J. M. Salman. Optimization of preparation conditions for activated carbon from palm oil fronds using response surface methodology on removal of pesticides from aqueous solution. Arabian Journal of Chemistry, Vol.7, 101–108, 2014. doi: 10.1016/j.arabjc.2013.05.033.

[24] T. D. Pham, T. T. Bui, V. T. Nguyen, T. K. Bui, T. N. Van, T.T. Tran. Adsorption of Polyelectrolyte onto Nano silica Synthesized from Rice Husk: Characteristics, mechanisms, and application for antibiotic removal. Polymers, Vol. 10, No. 2, 220, 2018. doi: 10.3390/polym10020220.

[25] P. D. Van, C. L. Ngoc, L. Anh Tuyet, N. Q. Hung, V. D. Nguyen, T. N. Ngoc. Insight into adsorption machanism of lead(II) from aqueous solution by chitosan loaded MnO2 nanoparticles. Material chemistry and physics, 207, 294-302, 2018. https://doi.org/10.1016/j.matchemphys.2017.12.071

[26] N. Kayal, P. K. Sinhia, D. Kundu. Application of chemically modified rice husk for the removal of heavy metals from aqueous solution. Journal of Environmental Science Engineering, Vol. 52, No. 1, 15-8, 2010. PMID: 21114100.

[27] H. S. Kusuma, H, M. Mahfud. Response Surface Methodology for Optimization Studies of Microwave-assisted Extraction of Sandalwood Oil. Journal of Materials and Environmental Science, 7, 1958–1971, 2016.

[28] J. U. A. U. C. Okoro, L. E. A. O. D. Onukwuli, I. O. O. K. G. Akpomie. Application of response surface methodology for optimization of dissolved solids adsorption by activated coal. Applied Water Science, 9, 1–11, 2019. doi: 10.1007/s13201-019-0943-7.

[29] L. Brahmi, F. Kaouah, S. Boumaza, M. Trari. Response surface methodology for the optimization of acid dye adsorption onto activated carbon prepared from wild date stones. Applied Water Science, 9, 1–13, 2019 doi: 10.1007/s13201-019-1053-2.

[30] M. Amini, H. Younesi, N. Bahramifar, A. Akbar, Z. Lorestani, F. Ghorbani, A. Daneshi, M. Sharifzadeh. Application of response surface methodology for optimization of lead biosorption in an aqueous solution by Aspergillus niger. Journal of Hazardous Materials, 154, 694–702, 2008. doi: 10.1016/j.jhazmat.2007.10.114.

[31] V. Javanbakht, S. M. Ghoreishi. Application of response surface methodology for optimization of lead removal from an aqueous solution by a novel superparamagnetic nanocomposite. Adsorption Science and Technology, 2017. doi: 10.1177/0263617416674474.

[32] M. S. Samuel, E. A. A. M, R. Chidambaram. Isotherm Modelling, Kinetic Study and Optimization of Batch Parameters Using Response Surface Methodology for Effective Removal of Cr (VI) Using Fungal Biomass. PLOS ONE, 10(3), e0116884. doi: 10.1371/journal.pone.0116884

[33] J.N. Sahu, J. Acharya, B.C. Meikap. Optimization of production conditions for activated carbons from Tamarind wood by zinc chloride using response surface methodology. Bioresource Technology, Vol 101, No.6, 1974-1982, 2010.

[34] A. Bazrafshan, S. Hajati, M. Ghaedi. Synthesis of regenerable $Zn(OH)_2$ nanoparticle-loaded activated carbon for the ultrasound-assisted removal of malachite green: optimization, isotherm, and kinetics. RSC advances, Vol 5, No.96, 79119-79128, 2015.

[35] H. Haroon, S. M. H. Gardazi, S. M. H, T. A. Butt, A. Pervez, Q. Mahmood, M. Bilal. Novel lignocellulosic wastes for comparative adsorption of Cr(VI): Equilibrium kinetics and thermodynamic studies. Polish Journal of Chemical

Techology, 19, 6–15, 2017. doi: 10.1515/pjct-2017-0021.

[36] W. Zou, R. Han, Z. Chen, J. Shi, L. Hongmin. Characterization and properties of manganese oxide coated zeolite as adsorbent for removal of copper (II) and lead (II) ions from solution. Journal of Chemical & Engineering Data, 51, 534–541, 2006. doi: 10.1021/je0504008.

[37] N. Boujelben, J. Bouzid, Z. E. Laboratoire, E. Energie, D. Génie. Removal of Lead (II) Ions from Aqueous Solutions Using Manganese Oxide-coated Adsorbents: Characterization and Kinetic Study. Adsorption Science and Technology, 177–191, 2009.

[38] N. K. Hamadi, X. D. Chen, M. M. Farid, M. G. Q. Lu. Adsorption kinetics for the removal of chromium (VI) from aqueous solution by adsorbents derived from used tyres and sawdust. Chemical Engineering Journal, Vol. 84, No. 15, 95-105, 2001. https://doi.org/10.1016/S1385-8947(01)00194-2.

[39] K. Kalantari, M. B. Ahmad, H. Reza, F. Masoumi, K. Shameli. Rapid Adsorption of Heavy Metals by Fe3O4/Talc Nanocomposite and Optimization Study Using Response Surface Methodology. International Journal Molecular Science, Vol. 15, No. 7, 12913–12927, 2014. doi: 10.3390/ijms150712913.

[40] S. R. Sivakkumar, J. Myoun, D. Young, B. C. Kim, G. G. Wallace. Performance evaluation of CNT/polypyrene/MnO2 composite electrodes for electrochemical capacitors. Electrochimica Acta, Vol. 52, No. 25, 7377–7385, 2007. doi: 10.1016/j.electacta.2007.06.023.

[41] D. Kalderis, S. Bethanis, P. Paraskeva, E. Diamadopoulos. Production of activated carbon from bagasse and rice husk by a single-stage chemical activation method at low retention times. Bioresource Technology, 99, 6809-6816, 2008. https://doi.org/10.1016/j.biortech.2008.01.041.

[42] V. N. Tirtom, A. Dinçer, S. Becerik, T. Aydemir, A. Çelik. Removal of lead (II) ions from aqueous solution by using crosslinked chitosan-clay beads. Desalination and Water Treatment, 39, 76-82, 2012. https://doi.org/10.1080/19443994.2012.669161.

[43] T. A. Saleh. Nanocomposite of carbon nanotubes/silica nanoparticles and their use for adsorption of Pb(II): from surface properties to sorption mechanism. Desalination and Water Treatment, 57, 10730-10744, 2016. https://doi.org/10.1080/19443994.2015.1036784.

[44] H. A. Sani, M. B. Ahmad, T. A. Saleh. Synthesis of zinc oxide/talc nanocomposite for enhanced lead adsorption from aqueous solutions. RSC Advances, 6, 108819-108827, 2016.

[45] M. W. Wan, C. C. Kan, B. D. Rogel, M. L. P. Dalida. Adsorption of copper (II) and lead (II) ions from aqueous solution on chitosan-coated sand. Carbohydrate Polymers, 80, 891-899, 2010.